Original Article

Investigation of the effects of miniscrew-assisted rapid palatal expansion on airflow in the upper airway of an adult patient with obstructive sleep apnea syndrome using computational fluid-structure interaction analysis

Jae-Sik Hur[a]
Hyoung-Ho Kim[b]
Jin-Young Choi[c,d]
Sang-Ho Suh[b]
Seung-Hak Baek[a,d]

[a]Department of Orthodontics, School of Dentistry, Seoul National University, Seoul, Korea

[b]Department of Mechanical Engineering, Soongsil University, Seoul, Korea

[c]Department of Oral and Maxillofacial Surgery, School of Dentistry, Seoul National University, Seoul, Korea

[d]Dental Research Institute, School of Dentistry, Seoul National University, Seoul, Korea

Objective: The objective of this study was to investigate the effects of miniscrew-assisted rapid palatal expansion (MARPE) on changes in airflow in the upper airway (UA) of an adult patient with obstructive sleep apnea syndrome (OSAS) using computational fluid-structure interaction analysis. **Methods:** Three-dimensional UA models fabricated from cone beam computed tomography images obtained before (T0) and after (T1) MARPE in an adult patient with OSAS were used for computational fluid dynamics with fluid-structure interaction analysis. Seven and nine cross-sectional planes (interplane distance of 10 mm) in the nasal cavity (NC) and pharynx, respectively, were set along UA. Changes in the cross-sectional area and changes in airflow velocity and pressure, node displacement, and total resistance at maximum inspiration (MI), rest, and maximum expiration (ME) were investigated at each plane after MARPE. **Results:** The cross-sectional areas at most planes in NC and the upper half of the pharynx were significantly increased at T1. Moreover, airflow velocity decreased in the anterior NC at MI and ME and in the nasopharynx and oropharynx at MI. The decrease in velocity was greater in NC than in the pharynx. The airflow pressure in the anterior NC and entire pharynx exhibited a decrease at T1. The amount of node displacement in NC and the pharynx was insignificant at both T0 and T1. Absolute values for the total resistance at MI, rest, and ME were lower at T1 than at T0. **Conclusions:** MARPE improves airflow and decreases resistance in UA; therefore, it may be an effective treatment modality for adult patients with moderate OSAS.
[Korean J Orthod 2017;47(6):353-364]

Key words: Miniscrew-assisted rapid palatal expansion, Obstructive sleep apnea syndrome, Computational fluid dynamics, Fluid-structure interaction

Corresponding author: Seung-Hak Baek.
Professor, Department of Orthodontics, Dental Research Institute, School of Dentistry, Seoul National University, 101 Daehak-ro, Jongno-gu, Seoul 03080, Korea.
Tel +82-2-2072-3952 e-mail drwhite@unitel.co.kr

INTRODUCTION

Obstructive sleep apnea syndrome (OSAS) is characterized by the temporary cessation of breathing (apnea) or shallow breathing (hypopnea) with decreased hemoglobin oxygen saturation.[1] On the basis of the etiology, severity, and collapse site in the upper airway (UA), various treatment modalities have been applied, such as weight reduction, continuous positive airway pressure therapy, intraoral appliance therapy, soft tissue procedures, and maxillomandibular advancement (MMA) surgery.[1-3]

Although conventional rapid palatal expansion (RPE) with tooth-borne anchorage has been suggested as a treatment option for OSAS, the subjects in most previous studies were children.[4-6] Because conventional RPE is thought to be less effective for adult patients, use of surgery-assisted RPE (SARPE) is recommended for adult patients with OSAS.[7-9] However, it has some disadvantages, including surgical invasiveness and a long retention period. Of late, miniscrew-assisted RPE (MARPE) has been receiving attention by clinicians because of increased orthopedic effects on expansion of the maxillary basal arch width when compared with conventional RPE.[10] Moreover, it induces noninvasive expansion of the midpalatal suture in adult patients, as opposed to SARPE.[11-13] Although MARPE is thought to be helpful for relieving the symptoms of OSAS in adult patients,[14,15] scientific evidence regarding its effects is limited.

Three-dimensional (3D) computational fluid dynamics (CFD) has been used to investigate airflow dynamics in patients with OSAS.[3,16-20] However, because UA, particularly the pharynx, is a deformable structure, adoption of fluid-structure interaction (FSI), which is a computational method to simulate flow and structural changes, has been recommended.[17,21] The use of FSI simulation can overcome the limitation of the rigid wall design in CFD and provide more realistic results compared with CFD.[17,21]

Despite the important anatomical and physiological roles of the nasal cavity (NC) in respiration, most numerical airflow simulation studies have omitted this structure during the fabrication of 3D airway models because of the complex structure and diverse shape as well as the computational cost of airflow simulation.[16-20] To investigate the effects of MARPE on the airflow dynamics in UA, NC must be included in 3D-computational modeling and FSI analysis.[22,23] From these perspectives, we conducted the present study to investigate the effects of MARPE on airflow in UA of an adult patient with OSAS using 3D-CFD/FSI analysis.

MATERIALS AND METHODS

Geometric modeling

For the fabrication of geometric models, a male patient with OSAS aged 18 years and 7 months was selected. The patient presented with a narrow maxillary basal arch and severe crowding and refused to use an intraoral appliance or undergo MMA surgery. Accordingly, MARPE was selected as the treatment method. Before the initiation of MARPE, he underwent an in-laboratory polysomnography study (age, 18 years and 7 months; body mass index [BMI], 25.0 kg/m^2; apnea and hypopnea index [AHI], 49.5 events/hour; respiratory disturbance index [RDI], 52.2 events/hour; lowest O_2 saturation rate [LSR], 85%). After the completion of MARPE at S-plant Dental Hospital in Seoul, Korea, his signs and symptoms of OSAS significantly resolved (age, 19 years and 1 month; BMI, 24.9 kg/m^2; AHI, 2.2 events/hour; RDI, 20.2 events/hour; LSR, 95%). This study was reviewed and approved by the Institutional Review Board of the School of Dentistry Seoul National University, Seoul, Korea (S-D20170001).

Cone-beam computed tomography (CBCT) was performed (3D eXam; Imaging Sciences International, Hatfield, PA, USA) before (T0) and 6 months after (T1) MARPE using the following parameters: volume size, 23-cm diameter × 17-cm height; resolution, 0.3 voxel; exposure conditions, 37.1 mA and 120 kVp for 17.8 seconds. Although there is no standardized method for setting the head and tongue posture during 3D image acquisition, CBCT was performed using the natural head posture and the letter "N" tongue posture in the present study. For the letter "N" tongue posture, the patient was instructed to place the tongue on the roof of the mouth, directly behind the anterior teeth without pressing against them, and purse the lips together.[24]

Digital imaging and communications in medicine (DICOM) data obtained at the T0 and T1 stages were exported to ICEM-CFD (ver. 15; ANSYS Inc., Canonsburg, PA, USA) to fabricate the surface model (STL file). Then,

Table 1. Numbers of nodes and elements before (T0) and 6 months after (T1) MARPE in the three-dimensional upper airway models of an adult patient with obstructive sleep apnea syndrome

Variable	T0 (n)		T1 (n)	
	Nodes	Elements	Nodes	Elements
CFD	56,558	251,893	59,495	265,830
FSI	1,522,662	6,659,746	139,251	723,473

MARPE, Miniscrew-assisted rapid palatal expansion; CFD, computational fluid dynamics; FSI, fluid-structure interaction.
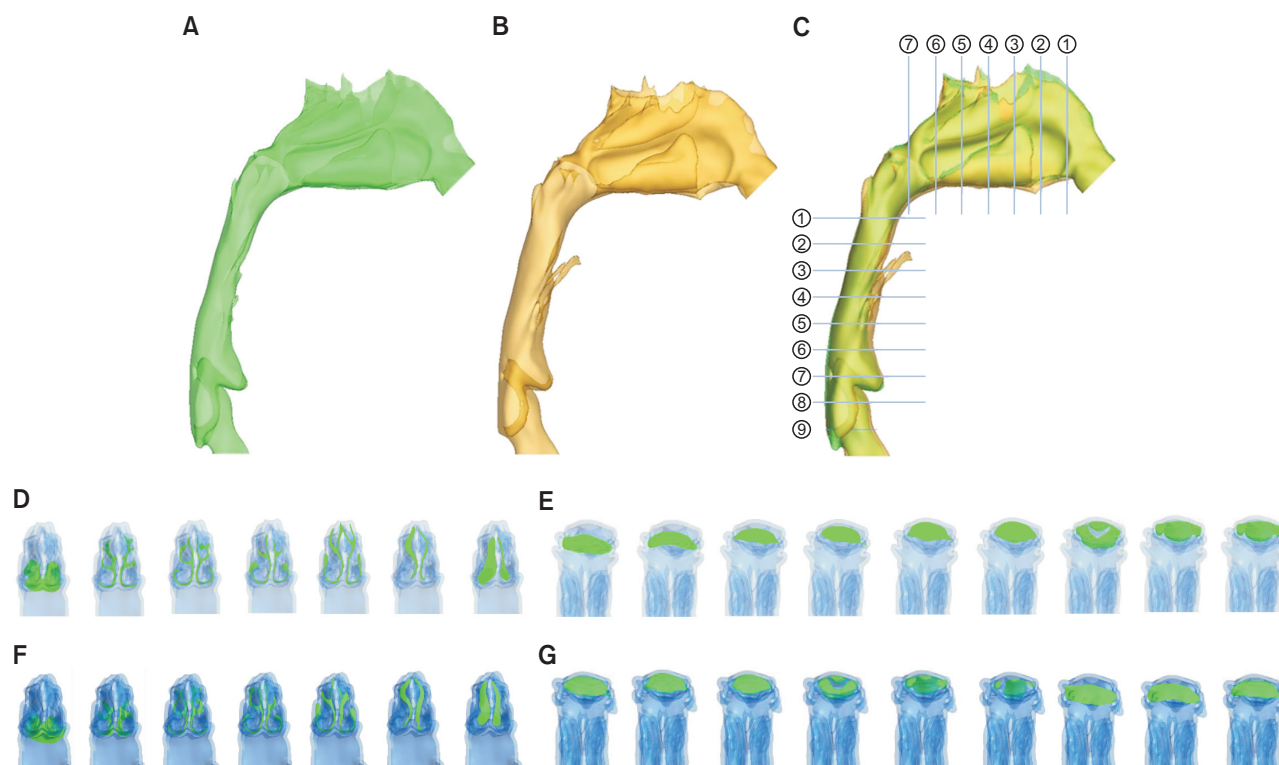
Figure 1. Three-dimensional models of the upper airway. T0 (**A**, green), T1 (**B**, yellow) and superimposition (**C**) of the models showing the locations of seven planes in the nasal cavity and nine planes in the pharynx. The superimposition was performed with the best-fit method using the anterior cranial base of T0 and T1 models, making the other structures invisible, then showing the upper airway only. Comparison of the cross sectional airway area between T0 (**D** and **E**) and T1 (**F** and **G**) at sections from ① to ⑦ in nasal cavity (D and F, from left to right) and from ① to ⑨ in Pharynx (E and G, from left to right).
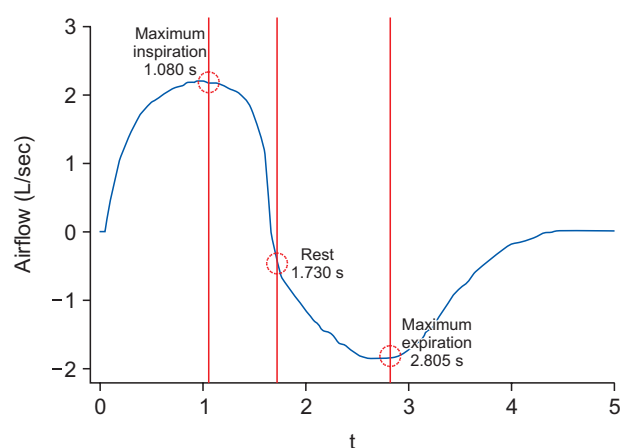

Figure 2. Respiratory cycle used for fluid-structure interaction simulation to investigate the effects of mini-screw-assisted rapid palatal expansion on the upper airway airflow in an adult patient with obstructive sleep apnea syndrome. Total duration of one cycle, 5 seconds. Maximum inspiration at 1.080 seconds, rest at 1.730 seconds, and maximum expiration at 2.805 seconds.

3D computational models of UA, including NC and the pharynx, were constructed. The meshes were generated with tetrahedron and prism elements. The total number of nodes and elements in each model is summarized in Table 1.

Computational FSI simulation

FSI simulation of UA was performed under the following conditions: boundary conditions, atmospheric pressure for the inlet and a regular respiration pattern (quantity/time) for the outlet; material properties, Young's modulus of 7,540 Pa and Poisson's ratio of 0.45[25]; seven planes in the NC area, with an interplane distance of 10 mm from the aperture of the nostril to the beginning of the pharynx (Figure 1); and nine planes in the pharynx area, with an interplane distance of 10 mm from the beginning of the pharynx to the beginning of the larynx (Figure 1). The respiratory cycle used during simulation is described in Figure 2.

For airflow simulation, the flow was assumed to be incompressible. The governing differential equations, the Reynolds-averaged Navier–Stokes equation for

turbulence with the k - ε model, and constitutive equations for structure dynamics are shown in Table 2. Constant air density (1.185 kg/m³) and viscosity (1.831 × 10⁻⁵ kg/m·s) values were assumed. No-slip wall boundary conditions were imposed on the airway walls.

The cross-sectional airway area at each plane was assessed at T0 and T1. In addition, airflow pressure and velocity, node displacement in the soft tissue of the airway wall, and the average pressure, the flow rate, and the total resistance were measured at maximum inspiration (MI), rest, and maximum expiration (ME) at both time points. Changes in the total resistance of airflow were calculated on the basis of changes in each variable from T0 to T1.

RESULTS

Changes in the cross–sectional airway area (Table 3)

In NC, the cross-sectional area at planes 1 to 3 showed a significant increase (range of increase: 0.96 cm² to 1.16 cm², 38.5% to 53.3%) at T1 compared with that at T0, while the area at planes 4 to 6 showed a moderate increase (0.65 cm² to 1.04 cm², 27.5% to 38.8%) and the area at plane 7 showed a slight increase. In the pharynx, a strong increasing trend was observed at planes 1 to 4 (1.39 cm² to 1.69 cm², 40.4% to 67.3%); this trend weakened at planes 5 and disappeared at planes 6 to 9. These findings imply that MARPE primarily affected the anterior and middle parts of NC, the nasopharynx (planes 1 and 2) and the upper and middle part of the oropharynx (planes 3, 4, and 5). The amount of increase in the cross-sectional airway area was larger for the pharynx than for NC, even though the pharynx was located farther than NC from

the MARPE appliance.

Changes in the pressure and velocity of airflow (Tables 4 and 5, Figures 3 and 4)

At planes 1 to 7 in NC and planes 1 to 5 in the pharynx, the absolute values for airflow pressure and velocity at MI, rest, and ME were lower at T1 than at T0.

In NC, airflow pressure and velocity at MI showed a significant decrease at planes 1 to 4 and planes 1, 2, 3, and 7, respectively, after MARPE (pressure: −29.3 Pa to −10.2 Pa, −52.9% to −33.3%; velocity: −0.98 m/s to −1.44 m/s; −29.9% to −37.9%). At rest, there was a slight decrease in pressure and no significant change in velocity at all seven planes. At ME, there was a decrease in pressure at planes 1 to 7 (26.2 Pa to 2.8 Pa, −53.6% to −17.5%) and a decrease in velocity at planes 1 to 3 (−0.87 m/s to −1.54 m/s; −35.9% to −42.6%).

In the pharynx, at MI, there was a considerable decrease in pressure at planes 1 to 7 (−9.6 Pa to −10.8 Pa; −34.1% to −37.0%) and a significant decrease in pressure at planes 8 (−12.6 Pa, −66.9%) and 9 (−13.5 Pa, −67.5%). Velocity showed a significant decrease at planes 1 to 4 (−0.61 m/s to −1.01 m/s; −31.1% to −41.3%), a moderate decrease at planes 5 to 7, and no significant change at planes 8 and 9. At rest, there were no significant changes in pressure and velocity at any of the nine planes. At ME, there was a steady pressure drop at planes 1 to 7 and a substantial drop at planes 8 (9.4 Pa, −73.9%) and 9 (8.9 Pa, −68.9%). Velocity also decreased at planes 1 through 5.

Table 2. The governing equations for numerical turbulence model

Category	Equation*
Differential equation	$\dfrac{\partial u_i}{\partial x_i} = 0$ $\rho \dfrac{\partial u_i}{\partial t} + u_j \dfrac{\partial u_i}{\partial x_j} = -\dfrac{\partial p}{\partial x_i} + \dfrac{\partial}{\partial x_j}[\mu_{eff}(\dfrac{\partial u_i}{\partial x_j} + \dfrac{\partial u_j}{\partial x_i}) - \rho \overline{u'_i u'_j}]$
Reynolds-averaged Navier–Stokes equation with the k - ε model	$\mu_{eff} = \mu + \mu_t,\ \mu_t = C_\mu \rho \dfrac{k^2}{\varepsilon}$ $\dfrac{\partial(\rho k)}{\partial t} + \dfrac{\partial(\rho k u_j)}{\partial x_j} = \dfrac{\partial}{\partial x_j}[(\mu + \dfrac{\mu_t}{\sigma_k})\dfrac{\partial k}{\partial x_j}] + P_k - \rho \varepsilon + P_{kb}$ $\dfrac{\partial(\rho \varepsilon)}{\partial t} + \dfrac{\partial(\rho \varepsilon u_j)}{\partial x_j} = \dfrac{\partial}{\partial x_j}[(\mu + \dfrac{\mu_t}{\sigma_\varepsilon})\dfrac{\partial \varepsilon}{\partial x_j}] + \dfrac{\varepsilon}{k}(C_{\varepsilon1} P_k - C_{\varepsilon2} \rho \varepsilon + C_{\varepsilon1} P_{\varepsilon b})$
Constitutive equation	$\rho a_i = \sigma_{ij,j} + \rho f_i,\ \sigma_{ij} = D_{ijkl} \varepsilon_{kl}$ $a_i = \dfrac{d\hat{u}_i}{dt},\ \sigma_{ij} n_i = T_i$

*Where t is the time on the structure domain, n_i is the unit outward pointing normal on the wall surface, T_i is the surface traction vector at time t, σ_{ij} is the mechanical stress tensor, D_{ijkl} is the Lagrangian elasticity tensor, and ε_{kl} is the strain tensor.

Table 3. Changes in the cross-sectional airway area in the nasal cavity and pharynx after MARPE in an adult patient with obstructive sleep apnea syndrome

Variable	Airway area (cm²)			
	Before MARPE (T0)	After MARPE (T1)	ΔT1–T0	Percentage of change [(ΔT1–T0)/T0] × 100
Nasal cavity				
Plane 1	2.49	3.44	0.96	38.51
Plane 2	1.63	2.48	0.86	52.62
Plane 3	2.17	3.33	1.16	53.27
Plane 4	2.33	2.98	0.65	27.98
Plane 5	2.57	3.27	0.71	27.51
Plane 6	2.69	3.73	1.04	38.78
Plane 7	5.54	6.13	0.58	10.54
Pharynx				
Plane 1	3.43	4.82	1.39	40.42
Plane 2	2.95	4.64	1.69	57.41
Plane 3	2.51	4.20	1.69	67.28
Plane 4	2.80	4.48	1.69	60.22
Plane 5	3.24	4.28	1.04	31.92
Plane 6	3.73	4.10	0.36	9.70
Plane 7	4.77	4.75	−0.02	−0.32
Plane 8	4.36	4.54	0.18	4.10
Plane 9	3.72	3.75	0.03	0.89

MARPE, Miniscrew-assisted rapid palatal expansion.

Changes in node displacement in the soft tissue of the airway wall (Table 6 and Figure 5)

In both NC and the pharynx, the node displacement value showed a decreasing pattern from MI to rest and an increasing pattern from rest to ME, particularly after MARPE. However, there was no clinically meaningful change in the absolute values, regardless of the respiration stage. These findings indicate that the changes in airflow pressure and velocity (Tables 4 and 5) did not affect node displacement in both NC and the pharynx (Table 6).

Changes in the average pressure, flow rate, and total resistance (Table 7)

Considering the significant decrease in the average pressure at MI (−55.5%), rest (−49.7%), and ME (−52.6%) from T0 to T1, the total resistance also exhibited a significant decrease at MI (−55.1%), rest (−35.9%), and ME (−33.9%).

DISCUSSION

In the present study, we investigated the effects of MARPE on airflow in UA of an adult patient with OSAS

using 3D-CFD/FSI analysis. The findings are discussed in detail as follows.

Changes in the cross-sectional airway area

The amount of increase in the cross-sectional airway area after MARPE was significantly larger in the anterior NC than in the posterior NC (Table 3). The increase extended below to the oropharynx (planes 1, 2, and 3) and the upper part of the laryngopharynx (planes 4 and 5; Table 3). Because of the anatomical continuity of NC and the pharynx, transverse expansion of the hard palate through MARPE can directly and indirectly increase the cross-sectional airway area at the NC and pharynx, respectively. These results are in agreement with those of previous studies that reported enlargement of the pharyngeal airway after conventional RPE in children[26] and SARPE in adults.[9]

The amount of increase in the cross-sectional area was larger for the pharynx than for NC (Table 3). We believe this was because of the complex structure of NC, which primarily comprises hard tissues such as the nasal septum, conchae, and palatal bone. On the other hand, the pharynx is a relatively simple tubing system made of soft tissue.

Table 4. Changes in airflow pressure in the nasal cavity and pharynx after MARPE in an adult patient with obstructive sleep apnea syndrome

| Variable | Pressure (Pa) | | | | | | ΔT1−T0 | | | Percentage of change [(ΔT1−T0)/T0] × 100 | | |
| | Before MARPE (T0) | | | After MARPE (T1) | | | | | | | | |
	Max. inspiration	Rest	Max. expiration	Max. inspiration	Rest	Max. expiration	Max. inspiration	Rest	Max. expiration	Max. inspiration	Rest	Max. expiration
Nasal cavity												
Plane 1	55.45	−6.77	−48.81	26.13	−3.46	−22.65	−29.32	3.31	26.16	−52.88	−48.87	−53.60
Plane 2	45.82	−6.07	−45.17	24.62	−3.21	−21.47	−21.20	2.86	23.70	−46.27	−47.06	−52.47
Plane 3	35.92	−4.56	−32.98	21.75	−2.76	−19.15	−14.17	1.81	13.83	−39.45	−39.58	−41.94
Plane 4	30.54	−3.50	−24.96	20.38	−2.42	−17.51	−10.16	1.07	7.45	−33.27	−30.69	−29.85
Plane 5	29.58	−2.75	−20.51	19.98	−1.99	−15.44	−9.60	0.76	5.07	−32.45	−27.52	−24.72
Plane 6	29.33	−2.24	−17.78	19.29	−1.69	−13.93	−10.04	0.55	3.85	−34.23	−24.68	−21.65
Plane 7	28.78	−1.98	−16.05	18.56	−1.54	−13.25	−10.22	0.45	2.80	−35.51	−22.58	−17.45
Pharynx												
Plane 1	29.28	−1.90	−16.05	18.45	−1.44	−13.25	−10.83	0.46	2.80	−36.99	−24.17	−17.45
Plane 2	29.01	−1.85	−16.51	18.54	−1.38	−13.20	−10.47	0.47	3.31	−36.09	−25.53	−20.05
Plane 3	27.97	−1.75	−16.78	18.42	−1.33	−13.19	−9.55	0.42	3.59	−34.14	−24.14	−21.40
Plane 4	28.03	−1.62	−16.77	18.42	−1.27	−13.10	−9.61	0.35	3.67	−34.29	−21.42	−21.88
Plane 5	28.42	−1.52	−16.81	18.34	−1.24	−13.49	−10.08	0.29	3.32	−35.47	−18.84	−19.75
Plane 6	28.76	−1.51	−17.18	18.20	−1.26	−13.89	−10.56	0.25	3.29	−36.72	−16.80	−19.15
Plane 7	25.38	−1.40	−15.39	14.64	−1.15	−12.10	−10.74	0.25	3.29	−42.32	−17.68	−21.38
Plane 8	18.86	−0.81	−12.72	6.25	−0.40	−3.33	−12.61	0.41	9.39	−66.86	−50.33	−73.85
Plane 9	19.99	−0.98	−12.84	6.51	−0.42	−4.00	−13.49	0.56	8.85	−67.46	−57.12	−68.89

MARPE, Miniscrew-assisted rapid palatal expansion.
Maximum (Max.) inspiration, 1.080 seconds; Rest, 1.730 seconds; Max. expiration, 2.805 seconds.

Table 5. Changes in airflow velocity (Max. inspiration, rest, and Max. expiration) in the nasal cavity and pharynx after MARPE in an adult patient with obstructive sleep apnea syndrome

Variable	Velocity (m/s)						ΔT1-T0			Percentage of change [(ΔT1-T0)/T0] × 100		
	Before MARPE (T0)			After MARPE (T1)								
	Max. inspiration	Rest	Max. expiration	Max. inspiration	Rest	Max. expiration	Max. inspiration	Rest	Max. expiration	Max. inspiration	Rest	Max. expiration
Nasal cavity												
Plane 1	3.28	0.70	3.22	2.30	0.49	1.85	−0.98	−0.21	−1.37	−29.93	−30.29	−42.64
Plane 2	3.89	0.86	3.65	2.45	0.54	2.11	−1.44	−0.33	−1.54	−37.00	−37.82	−42.25
Plane 3	2.90	0.63	2.42	1.80	0.41	1.56	−1.10	−0.22	−0.87	−37.93	−35.38	−35.85
Plane 4	2.61	0.58	2.22	1.98	0.45	1.70	−0.63	−0.14	−0.52	−23.98	−23.10	−23.31
Plane 5	2.40	0.53	2.04	1.83	0.43	1.60	−0.56	−0.11	−0.44	−23.53	−20.57	−21.64
Plane 6	2.76	0.55	2.07	1.77	0.40	1.54	−0.99	−0.15	−0.54	−35.71	−27.05	−25.95
Plane 7	2.06	0.35	1.29	1.47	0.31	1.25	−0.58	−0.05	−0.05	−28.34	−12.79	−3.49
Pharynx												
Plane 1	1.96	0.40	1.62	1.35	0.32	1.24	−0.61	−0.09	−0.38	−31.14	−21.83	−23.57
Plane 2	2.20	0.47	1.90	1.35	0.30	1.31	−0.85	−0.16	−0.59	−38.64	−34.91	−31.13
Plane 3	2.45	0.53	2.14	1.44	0.32	1.52	−1.01	−0.21	−0.62	−41.30	−39.15	−28.93
Plane 4	2.16	0.48	1.98	1.33	0.31	1.56	−0.83	−0.17	−0.42	−38.27	−35.30	−21.34
Plane 5	1.84	0.41	1.79	1.38	0.33	1.66	−0.46	−0.08	−0.12	−25.14	−20.16	−6.83
Plane 6	1.63	0.40	1.69	1.46	0.39	1.86	−0.17	−0.01	0.17	−10.55	−2.24	9.76
Plane 7	2.30	0.39	1.96	2.02	0.40	2.19	−0.28	0.01	0.23	−12.14	3.60	11.77
Plane 8	2.07	0.42	2.18	2.07	0.38	1.64	−0.01	−0.03	−0.54	−0.29	−7.69	−24.67
Plane 9	2.88	0.44	1.94	3.02	0.39	1.59	0.14	−0.06	−0.35	4.68	−12.94	−17.93

MARPE, Miniscrew-assisted rapid palatal expansion.
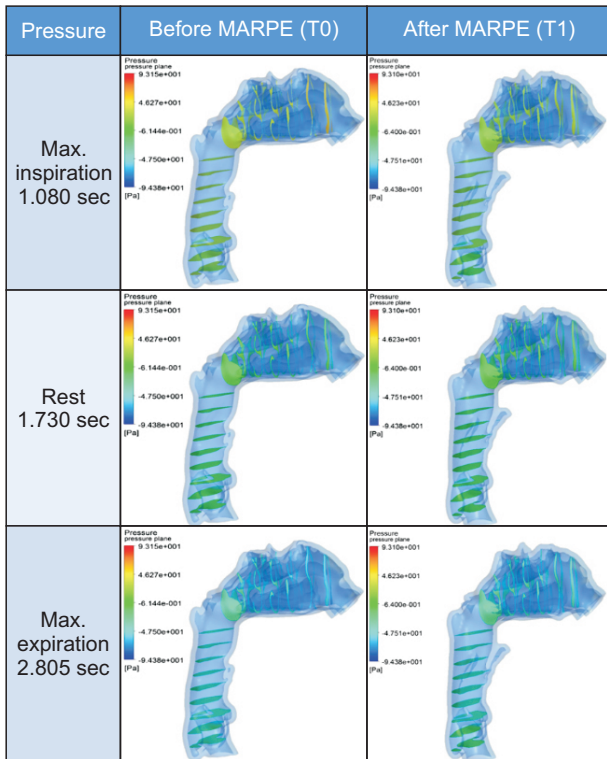Maximum (Max.) inspiration, 1.080 seconds; Rest, 1.730 seconds; Max. expiration, 2.805 seconds.

Figure 3. Changes in airflow pressure in the nasal cavity and pharynx at maximum (Max.) inspiration, rest, and Max. expiration after miniscrew-assisted rapid palatal expansion (MARPE) in an adult patient with obstructive sleep apnea syndrome.
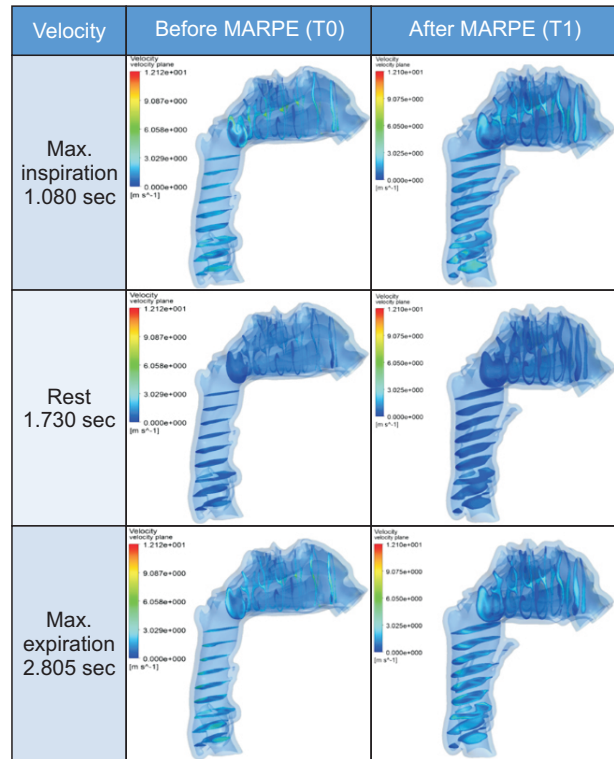
Figure 4. Changes in airflow velocity in the nasal cavity and pharynx at maximum (Max.) inspiration, rest, and Max. expiration after miniscrew-assisted rapid palatal expansion (MARPE) in an adult patient with obstructive sleep apnea syndrome.

Changes in airflow pressure and velocity

After MARPE, we found a pressure drop in NC and the pharynx at MI and ME. A decrease in airflow velocity existed primarily in the anterior NC at both ME and MI and the oropharynx (planes 1 to 3) and upper part of the laryngopharynx (planes 4 and 5) at MI (Tables 4 and 5, Figures 3 and 4). Although NC exhibited a smaller increase in the cross-sectional airway area compared with the pharynx (Table 3), the former exhibited a greater decrease in both pressure and velocity compared with the pharynx. This was probably because the anterior NC plays an important role as the main entrance and exit for airflow and decreases the airflow resistance in UA (Tables 4 and 5). The impact of NC expansion may extend to the middle part of the oropharynx (Tables 4 and 5, Figures 3 and 4). These results are in accordance with those of Iwasaki et al.[22] However, their study modeled only NC; therefore, their data cannot be generalized to the entire process of respiration.

Because the differences in pressure and velocity between inspiration and expiration decreased after MARPE (Tables 4 and 5, Figures 3 and 4), it can be stated that MARPE smoothened the airflow gradient and improved the respiration quality.

Changes in node displacement in the soft tissue of the airway wall

The amount of node displacement in both NC and the pharynx was too small to be considered clinically meaningful (Table 6 and Figure 5). This finding was not concordant with that in a previous FSI study by Zhao et al.,[17] who reported that the amount of node displacement in the pharynx appeared to be significant. This difference in findings may have resulted from the fact that we included NC in our 3D airway models, whereas Zhao et al.[17] excluded the same. Therefore, the findings from our study suggest that the airway wall in NC and the pharynx do not move during the respiratory cycle to the extent reported by Zhao et al.[17] In other words, the amounts of node displacement in the pharynx turned into insignificant when the nasal cavity was included in FSI analysis.

Changes in the average pressure, flow rate, and total resistance

In the present study, MARPE significantly decreased

Table 6. Changes in node displacement in the soft tissue of the airway wall (Max. inspiration, rest, and Max. expiration) after MARPE in an adult patient with obstructive sleep apnea syndrome

Variable	Displacement (mm)								
	Before MARPE (T0)			After MARPE (T1)			ΔT1–T0		
	Max. inspiration	Rest	Max. expiration	Max. inspiration	Rest	Max. expiration	Max. inspiration	Rest	Max. expiration
Nasal cavity									
Plane 1	1.48E-10	2.52E-11	1.24E-10	4.03E-10	8.89E-11	3.72E-10	2.55E-10	6.37E-11	2.48E-10
Plane 2	2.09E-10	4.13E-11	1.98E-10	6.82E-10	1.82E-10	6.56E-10	4.73E-10	1.41E-10	4.58E-10
Plane 3	2.55E-10	5.28E-11	2.38E-10	9.04E-10	2.36E-10	8.63E-10	6.49E-10	1.83E-10	6.25E-10
Plane 4	2.51E-10	5.86E-11	2.23E-10	9.66E-10	2.76E-10	9.09E-10	7.15E-10	2.17E-10	6.86E-10
Plane 5	2.11E-10	6.03E-11	1.65E-10	8.20E-10	2.77E-10	7.17E-10	6.09E-10	2.17E-10	5.52E-10
Plane 6	1.81E-10	6.38E-11	1.24E-10	6.46E-10	2.67E-10	4.73E-10	4.65E-10	2.03E-10	3.49E-10
Plane 7	1.61E-10	5.85E-11	7.25E-11	6.06E-10	2.25E-10	3.08E-10	4.45E-10	1.67E-10	2.36E-10
Pharynx									
Plane 1	3.03E-07	5.91E-08	1.35E-07	1.42E-06	3.11E-07	8.62E-07	1.12E-06	2.52E-07	7.27E-07
Plane 2	3.41E-07	6.23E-08	1.58E-07	1.74E-06	3.27E-07	1.09E-06	1.40E-06	2.65E-07	9.32E-07
Plane 3	3.20E-07	6.14E-08	1.53E-07	1.59E-06	2.75E-07	1.01E-06	1.27E-06	2.14E-07	8.57E-07
Plane 4	2.90E-07	5.59E-08	1.43E-07	1.48E-06	2.58E-07	9.62E-07	1.19E-06	2.02E-07	8.19E-07
Plane 5	2.62E-07	4.48E-08	1.37E-07	1.23E-06	1.97E-07	8.10E-07	9.68E-07	1.52E-07	6.73E-07
Plane 6	2.22E-07	3.11E-08	1.23E-07	8.73E-07	1.43E-07	5.91E-07	6.51E-07	1.12E-07	4.68E-07
Plane 7	1.22E-07	1.86E-08	6.60E-08	4.57E-07	1.06E-07	2.87E-07	3.35E-07	8.74E-08	2.21E-07
Plane 8	8.89E-08	1.52E-08	4.52E-08	3.11E-07	8.85E-08	1.61E-07	2.22E-07	7.33E-08	1.16E-07
Plane 9	4.70E-08	9.72E-09	2.08E-08	1.52E-07	5.29E-08	9.72E-08	1.05E-07	4.32E-08	7.64E-08

MARPE, Miniscrew-assisted rapid palatal expansion.
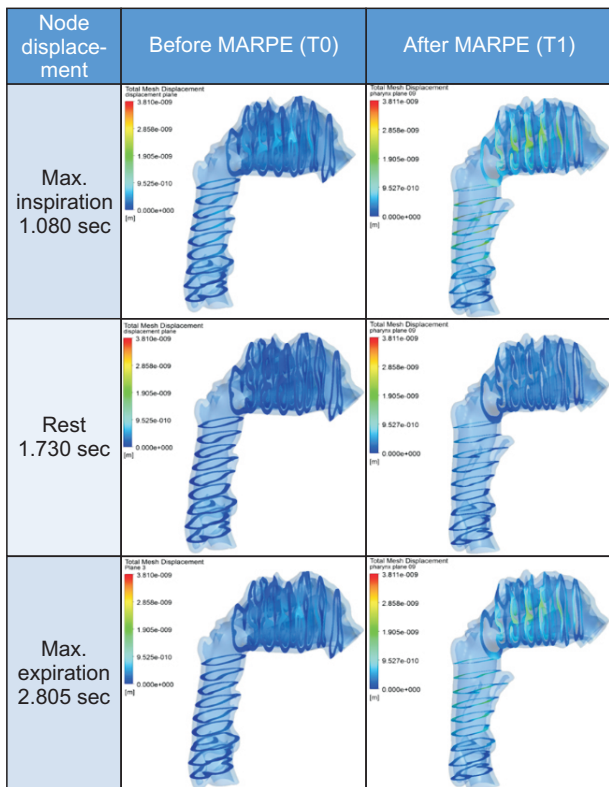Maximum (Max.) inspiration, 1.080 seconds; Rest, 1.730 seconds; Max. expiration, 2.805 seconds.

Figure 5. Changes in node displacement in the soft tissue of the airway wall at maximum (Max.) inspiration, rest, and Max. expiration after miniscrew-assisted rapid palatal expansion (MARPE) in an adult patient with obstructive sleep apnea syndrome.

the total resistance in UA during the entire respiratory cycle (Table 7). This finding is in accordance with that from a previous review,[27] which suggested that expansion of the NC floor can benefit patients with a constricted maxillary arch and nasal airflow problem.

Because we included NC in our 3D computational model and used FSI simulation, our results may reveal more realistic effects of MARPE on changes in the airflow of adult patients with OSAS compared with previous studies.[9,18,23,27] However, further studies will be needed to use CT data of OSAS patients taken in the supine position and to find more realistic values of material properties of the upper airway for better CFD/FSI model. And it should also be endeavored to investigate other treatment modalities for OSAS (e.g., intraoral appliance, soft tissue procedures, and MMA) with a large sample size.

CONCLUSION

Three-dimensional CFD/FSI analysis with an appropriate model incorporating NC and the pharynx showed

Table 7. Changes in the average pressure, flow rate, and total resistance (Max. inspiration, rest, and Max. expiration) after MARPE in an adult patient with obstructive sleep apnea syndrome

Variable	Before MARPE (T0)			After MARPE (T1)			ΔT1-T0			Percentage of change [(ΔT1-T0)/T0] × 100		
	Max. inspiration	Rest	Max. expiration	Max. inspiration	Rest	Max. expiration	Max. inspiration	Rest	Max. expiration	Max. inspiration	Rest	Max. expiration
Average pressure (Pa)	−69.2919	6.754787	38.9248	−30.8579	3.39817	18.46018	38.43398	−3.35662	−20.4646	−55.47	−49.69	−52.58
Flow rate (kg/s)	0.000684	0.000228	0.00106	0.000679	0.000179	0.000761	−0.000005	−0.000049	−0.000299	−0.73	−21.49	−28.21
Total resistance (1/m·s)	−101,304	29,626.26	36,721.51	−45,446.1	18,984.19	24,257.79	55,857.82	−10,642.1	−12,463.7	−55.14	−35.92	−33.94

MARPE, Miniscrew-assisted rapid palatal expansion.
Maximum (Max.) inspiration, 1.080 seconds; Rest, 1.730 seconds; Max. expiration, 2.805 seconds.
Adopting the electric current formula (R = V/I, where V is the voltage, I is the current, and R is the resistance), the resistance can be calculated using the following equation: R = P/Q, where P is the pressure, Q is the quantity of fluid current, and R is the resistance.

an improvement in airflow and a decrease in resistance in UA after MARPE.

MARPE can serve as an alternative treatment modality for adult patients with who have moderate to severe narrow basal arch and crowding and refuse to the intraoral appliance or MMA surgery.

REFERENCES

1. Ahn HW, Cho IS, Cho KC, Choi JY, Chung JW, Baek SH. Surgical treatment modality for facial esthetics in an obstructive sleep apnea patient with protrusive upper lip and acute nasolabial angle. Angle Orthod 2013;83:355-63.

2. Epstein LJ, Kristo D, Strollo PJ Jr, Friedman N, Malhotra A, Patil SP, et al. Clinical guideline for the evaluation, management and long-term care of obstructive sleep apnea in adults. J Clin Sleep Med 2009;5:263-76.

3. Kim T, Kim HH, Hong So, Baek SH, Kim KW, Suh SH, et al. Change in the upper airway of patients with obstructive sleep apnea syndrome using computational fluid dynamics analysis: Conventional maxillomandibular advancement versus modified maxillomandibular advancement with anterior segmental setback osteotomy. J Craniofac Surg 2015;26:e765-70.

4. Katyal V, Pamula Y, Daynes CN, Martin J, Dreyer CW, Kennedy D, et al. Craniofacial and upper airway morphology in pediatric sleep-disordered breathing and changes in quality of life with rapid maxillary expansion. Am J Orthod Dentofacial Orthop 2013;144:860-71.

5. Villa MP, Rizzoli A, Rabasco J, Vitelli O, Pietropaoli N, Cecili M, et al. Rapid maxillary expansion outcomes in treatment of obstructive sleep apnea in children. Sleep Med 2015;16:709-16.

6. Taddei M, Alkhamis N, Tagariello T, D'Alessandro G, Mariucci EM, Piana G. Effects of rapid maxillary expansion and mandibular advancement on upper airways in Marfan's syndrome children: a home sleep study and cephalometric evaluation. Sleep Breath 2015;19:1213-20.

7. Pereira-Filho VA, Monnazzi MS, Gabrielli MA, Spin-Neto R, Watanabe ER, Gimenez CM, et al. Volumetric upper airway assessment in patients with transverse maxillary deficiency after surgically assisted rapid maxillary expansion. Int J Oral Maxillofac Surg 2014;43:581-6.

8. Jaipal PR, Rachala MR, Rajan R, Jhawar DK, Ankush B. Management of adult transverse malocclusion with surgically assisted rapid palatal expansion. J Clin Diagn Res 2016y;10:ZJ10-2.

9. Vinha PP, Faria AC, Xavier SP, Christino M, de Mello-Filho FV. Enlargement of the pharynx resulting from surgically assisted rapid maxillary expansion. J Oral Maxillofac Surg 2016;74:369-79.

10. Park JJ, Park YC, Lee KJ, Cha JY, Tahk JH, Choi YJ. Skeletal and dentoalveolar changes after miniscrew-assisted rapid palatal expansion in young adults: A cone-beam computed tomography study. Korean J Orthod 2017;47:77-86.

11. Wilmes B, Nienkemper M, Drescher D. Application and effectiveness of a mini-implant- and tooth-borne rapid palatal expansion device: the hybrid hyrax. World J Orthod 2010;11:323-30.

12. Choi SH, Shi KK, Cha JY, Park YC, Lee KJ. Non-surgical miniscrew-assisted rapid maxillary expansion results in acceptable stability in young adults. Angle Orthod 2016;86:713-20.

13. Suzuki H, Moon W, Previdente LH, Suzuki SS, Garcez AS, Consolaro A. Miniscrew-assisted rapid palatal expander (MARPE): the quest for pure orthopedic movement. Dental Press J Orthod 2016;21:17-23.

14. Kabalan O, Gordon J, Heo G, Lagravère MO. Nasal airway changes in bone-borne and tooth-borne rapid maxillary expansion treatments. Int Orthod 2015;13:1-15.

15. Park JJ, Park YC, Lee KJ, Cha JY, Tahk JH, Choi YJ. Skeletal and dentoalveolar changes after miniscrew-assisted rapid palatal expansion in young adults: a cone-beam computed tomography study. Korean J Orthod 2017;47:77-86.

16. Mylavarapu G, Mihaescu M, Fuchs L, Papatziamos G, Gutmark E. Planning human upper airway surgery using computational fluid dynamics. J Biomech 2013;46:1979-86.

17. Zhao M, Barber T, Cistulli PA, Sutherland K, Rosengarten G. Simulation of upper airway occlusion without and with mandibular advancement in obstructive sleep apnea using fluid-structure interaction. J Biomech 2013;46:2586-92.

18. Pirnar J, Dolenc-Grošelj L, Fajdiga I, Žun I. Computational fluid-structure interaction simulation of airflow in the human upper airway. J Biomech 2015;48:3685-91.

19. Shah DH, Kim KB, McQuilling MW, Movahed R, Shah AH, Kim YI. Computational fluid dynamics for the assessment of upper airway changes in skeletal Class III patients treated with mandibular setback surgery. Angle Orthod 2016;86:976-82.

20. Liu SY, Huon LK, Iwasaki T, Yoon A, Riley R, Powell N, et al. Efficacy of maxillomandibular advancement examined with drug-induced sleep endoscopy and computational fluid dynamics airflow modeling. Otolaryngol Head Neck Surg 2016;154:189-95.

21. Cheng GC, Koomullil RP, Ito Y, Shih AM, Sittitavornwong S, Waite PD. Assessment of surgical

effects on patients with obstructive sleep apnea syndrome using computational fluid dynamics simulations. Math Comput Simul 2014;106:44-59.

22. Iwasaki T, Saitoh I, Takemoto Y, Inada E, Kanomi R, Hayasaki H, et al. Improvement of nasal airway ventilation after rapid maxillary expansion evaluated with computational fluid dynamics. Am J Orthod Dentofacial Orthop 2012;141:269-78.

23. Cisonni J, Lucey AD, King AJ, Islam SM, Lewis R, Goonewardene MS. Numerical simulation of pharyngeal airflow applied to obstructive sleep apnea: effect of the nasal cavity in anatomically accurate airway models. Med Biol Eng Comput 2015;53:1129-39.

24. Gurani SF, Di Carlo G, Cattaneo PM, Thorn JJ, Pinholt EM. Effect of head and tongue posture on the pharyngeal airway dimensions and morphology in three-dimensional imaging: a systematic review. J Oral Maxillofac Res 2016;7:e1.

25. Cheng S, Gandevia SC, Green M, Sinkus R, Bilston LE. Viscoelastic properties of the tongue and soft palate using MR elastography. J Biomech 2011; 44:450-4.

26. Iwasaki T, Saitoh I, Takemoto Y, Inada E, Kakuno E, Kanomi R, et al. Tongue posture improvement and pharyngeal airway enlargement as secondary effects of rapid maxillary expansion: a cone-beam computed tomography study. Am J Orthod Dentofacial Orthop 2013;143:235-45.

27. Neeley WW 2nd, Edgin WA, Gonzales DA. A review of the effects of expansion of the nasal base on nasal airflow and resistance. J Oral Maxillofac Surg 2007;65:1174-9.